多边曲面的理论与性质

朱春钢

大连理工大学 数学科学学院

CAD/CAE/CAM专题——CAD技术的新进展

2022年11月10日 GAMES

Outlines

Outlines

Rational Bézier curves

Definition

Given weights $\omega_i \geq 0 (\omega_0, \omega_n > 0)$ and control points $\mathbf{p}_i \in \mathbb{R}^3$, the parametric curve

$$\mathbf{P}(t) = \frac{\sum_{i=0}^{n} \mathbf{p}_i \omega_i B_i^n(t)}{\sum_{i=0}^{n} \omega_i B_i^n(t)}, \quad 0 \leq t \leq 1, \tag{1.1}$$

is called **rational Bézier curve** of degree n, where $B_i^n(t) = \binom{n}{i} t^i (1-t)^{n-i}$ are Bernstein basis functions.

Cubic Bézeir curves

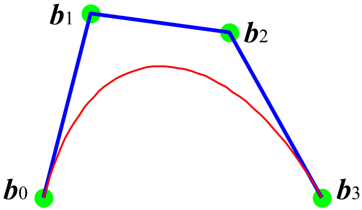

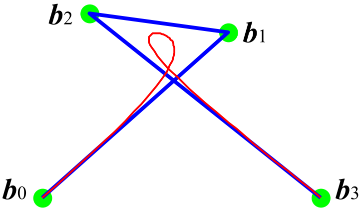

Tensor product and simplicial Bernstein basis functions

Tensor product Bernstein basis functions of degree $m \times n$

$$B_{i,j}^{m,n}(u,v) = B_i^m(u)B_j^n(v),$$
$$i = 0, 1, \cdots, m, j = 0, 1, \cdots, n.$$

Tensor product and simplicial Bernstein basis functions

Tensor product Bernstein basis functions of degree $m \times n$

$$B_{i,j}^{m,n}(u,v) = B_i^m(u) B_j^n(v),$$
$$i = 0, 1, \cdots, m, j = 0, 1, \cdots, n.$$

Simplicial Bernstein basis functions of degree n

$$B_{\boldsymbol{\lambda}}^n(\boldsymbol{\tau}) = \frac{n!}{\lambda!} \boldsymbol{\tau}^{\boldsymbol{\lambda}} = \frac{n!}{\lambda_1! \lambda_2!, \lambda_3!} \tau_1^{\lambda_1} \tau_2^{\lambda_2} \tau_3^{\lambda_3},$$
$$\boldsymbol{\lambda} = (\lambda_1, \lambda_2, \lambda_3), \quad \boldsymbol{\tau} = (\tau_1, \tau_2, \tau_3), |\boldsymbol{\lambda}| = n, |\boldsymbol{\tau}| = 1.$$

Tensor product and simplicial Bernstein basis functions

Tensor product Bernstein basis functions of degree $m \times n$

$$B_{i,j}^{m,n}(u,v) = B_i^m(u) B_j^n(v),$$
$$i = 0, 1, \cdots, m, j = 0, 1, \cdots, n.$$

Simplicial Bernstein basis functions of degree n

$$B_{\boldsymbol{\lambda}}^n(\boldsymbol{\tau}) = \frac{n!}{\lambda!} \boldsymbol{\tau}^{\boldsymbol{\lambda}} = \frac{n!}{\lambda_1! \lambda_2!, \lambda_3!} \tau_1^{\lambda_1} \tau_2^{\lambda_2} \tau_3^{\lambda_3},$$
$$\boldsymbol{\lambda} = (\lambda_1, \lambda_2, \lambda_3), \quad \boldsymbol{\tau} = (\tau_1, \tau_2, \tau_3), |\boldsymbol{\lambda}| = n, |\boldsymbol{\tau}| = 1.$$

Rational Bézier surfaces and volumes can be constructed by tensor product and simplicial Bernstein basis functions.

Rectangle Bézier surface, Bézier triangle, and Bézier volumes

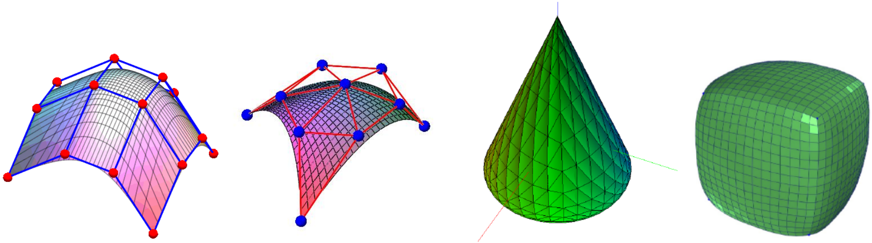

Multi-sided surfaces

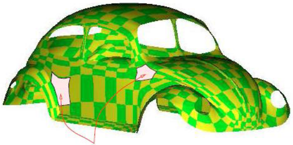

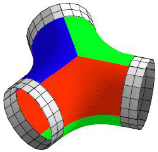

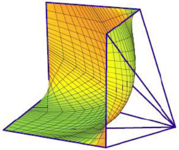

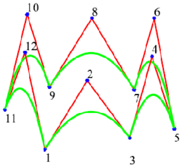

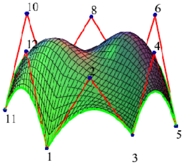

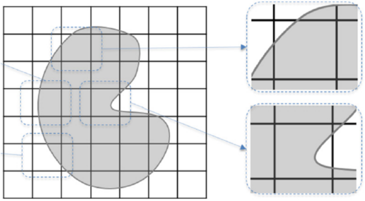

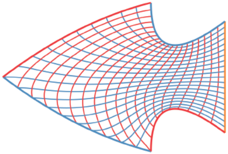

Multi-sided parametric surfaces

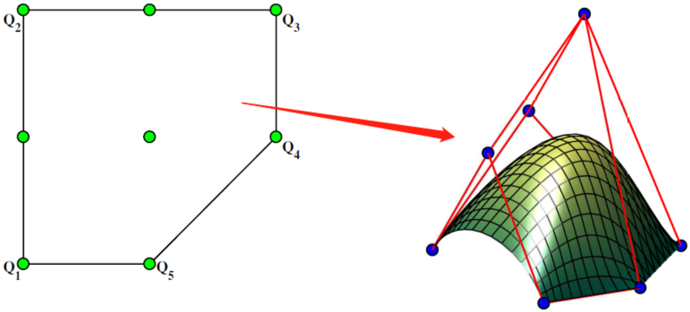

Methods for multi-sided surface construction

1. **N-sided surface patches**: J. A. Gregory, 1986.
2. **S-patches**: C. Loop and T. DeRose, 1989.
3. **Hexagonal patches**: J. Warren, 1992.
4. **Toric surface patches**: R. Krasauskas, 2002.
5. **M-surfaces**: K. Karčiauskas, 2003.
6. **Unstructured T-splines**: M. Scott, R. Simpson, J. Evans, S. Lipton, S. Bordas, T. Huges, 2013.
7. **Generalized (Multi-sided) Bézier surfaces**: T. Várady, P. Salvi, G. Karikó, 2016.
8. **Multi-sided B-spline surfaces**: M. Vaitkus, T. Várady, P. Salvi, Á. Sipos, 2021.
9. **TCB-splines**: J. Cao, Z. Chen, X. Wei, Y. J. Zhang, 2022.
10. **Subdivision-based methods, unstructured spline technologies, multi-patch methods,** $\cdots$

Outlines

Univariate Bernstein basis

Let $\mathcal{A} = \{0, 1, \cdots, n\}$ and

$$I_{\mathcal{A}} = conv(\mathcal{A}) = [0, n] = \{x \in \mathbb{R} \mid L_1(x) = x \geq 0, L_2(x) = n - x \geq 0\}.$$

Univariate Bernstein basis

Let $\mathcal{A} = \{0, 1, \cdots, n\}$ and

$$I_{\mathcal{A}} = conv(\mathcal{A}) = [0, n] = \{x \in \mathbb{R} \mid L_1(x) = x \geq 0, L_2(x) = n - x \geq 0\}.$$

For every $i \in \mathcal{A}$ and $c_i > 0$, define

$$\beta_i(x) := c_i L_1(x)^{L_1(i)} L_2(x)^{L_2(i)} = c_i x^i (n - x)^{(n-i)},$$

Univariate Bernstein basis

Let $\mathcal{A} = \{0, 1, \cdots, n\}$ and

$$I_{\mathcal{A}} = conv(\mathcal{A}) = [0, n] = \{x \in \mathbb{R} \mid L_1(x) = x \geq 0, L_2(x) = n - x \geq 0\}.$$

For every $i \in \mathcal{A}$ and $c_i > 0$, define

$$\beta_i(x) := c_i L_1(x)^{L_1(i)} L_2(x)^{L_2(i)} = c_i x^i (n - x)^{(n-i)},$$

If we set $x = nt, c_i = \binom{n}{i} n^{-n}$, then they are the classical univariate Bernstein basis functions of degree n.

Toric Bernstein basis

Let $\mathcal{A} \subset \mathbb{Z}^d$ be a finite set, $\sharp(\mathcal{A}) = n$, and

$$I_{\mathcal{A}} = conv(\mathcal{A}) = \{\mathbf{x} \in \mathbb{R}^d \mid 0 \le L_i(\mathbf{x}), i = 1, \ldots, N\}.$$

Toric Bernstein basis

Let $\mathcal{A} \subset \mathbb{Z}^d$ be a finite set, $\sharp(\mathcal{A}) = n$, and

$$I_{\mathcal{A}} = conv(\mathcal{A}) = \{\mathbf{x} \in \mathbb{R}^d \mid 0 \leq L_i(\mathbf{x}), i = 1, \ldots, N\}.$$

For every $\mathbf{a} \in \mathcal{A}$, define the toric Bernstein basis function

$$\beta_{\mathbf{a}}(\mathbf{x}) \ := c_{\mathbf{a}} L_1(\mathbf{x})^{L_1(\mathbf{a})} L_2(\mathbf{x})^{L_2(\mathbf{a})} \cdots L_N(\mathbf{x})^{L_N(\mathbf{a})},$$

where $c_{\mathbf{a}} > 0$.

Toric surface patches

Definition (Krasauskas, 2002)

Given $\mathcal{A} \subset \mathbb{Z}^d$, weights $\omega = \{\omega_{\mathbf{a}} \geq 0 | \mathbf{a} \in \mathcal{A}\}$ and control points $\mathcal{P} = \{\mathbf{P}_{\mathbf{a}} | \mathbf{a} \in \mathcal{A}\} \in \mathbb{R}^m$,

Toric surface patches

Definition (Krasauskas, 2002)

Given $\mathcal{A} \subset \mathbb{Z}^d$, weights $\omega = \{\omega_{\mathbf{a}} \geq 0 | \mathbf{a} \in \mathcal{A}\}$ and control points $\mathcal{P} = \{\mathbf{P}_{\mathbf{a}} | \mathbf{a} \in \mathcal{A}\} \in \mathbb{R}^m$, the parametric surface patch

$$\mathcal{B}_{\mathcal{A},\omega,\mathcal{P}}(\mathbf{x}) = \frac{\sum_{\mathbf{a}\in\mathcal{A}} \mathbf{P}_{\mathbf{a}} \omega_{\mathbf{a}} \beta_{\mathbf{a}}(\mathbf{x})}{\sum_{\mathbf{a}\in\mathcal{A}} \omega_{\mathbf{a}} \beta_{\mathbf{a}}(\mathbf{x})}, \qquad \mathbf{x} \in I_{\mathcal{A}}.$$

is called a **toric surface patch** (or toric Bézier patch, toric patch) defined in $\mathbb{R}^m$.

Toric surface patches

Definition (Krasauskas, 2002)

Given $\mathcal{A} \subset \mathbb{Z}^d$, weights $\omega = \{\omega_{\mathbf{a}} \geq 0 | \mathbf{a} \in \mathcal{A}\}$ and control points $\mathcal{P} = \{\mathbf{P}_{\mathbf{a}} | \mathbf{a} \in \mathcal{A}\} \in \mathbb{R}^m$, the parametric surface patch

$$\mathcal{B}_{\mathcal{A},\omega,\mathcal{P}}(\mathbf{x}) = \frac{\sum_{\mathbf{a}\in\mathcal{A}} \mathbf{P}_{\mathbf{a}}\omega_{\mathbf{a}}\beta_{\mathbf{a}}(\mathbf{x})}{\sum_{\mathbf{a}\in\mathcal{A}} \omega_{\mathbf{a}}\beta_{\mathbf{a}}(\mathbf{x})}, \qquad \mathbf{x} \in I_{\mathcal{A}}.$$

is called a **toric surface patch** (or toric Bézier patch, toric patch) defined in $\mathbb{R}^m$.

Why toric?

Toric surface patches

Definition (Krasauskas, 2002)

Given $\mathcal{A} \subset \mathbb{Z}^d$, weights $\omega = \{\omega_{\mathbf{a}} \geq 0 | \mathbf{a} \in \mathcal{A}\}$ and control points $\mathcal{P} = \{\mathbf{P}_{\mathbf{a}} | \mathbf{a} \in \mathcal{A}\} \in \mathbb{R}^m$, the parametric surface patch

$$\mathcal{B}_{\mathcal{A},\omega,\mathcal{P}}(\mathbf{x}) = \frac{\sum_{\mathbf{a}\in\mathcal{A}} \mathbf{P}_{\mathbf{a}} \omega_{\mathbf{a}} \beta_{\mathbf{a}}(\mathbf{x})}{\sum_{\mathbf{a}\in\mathcal{A}} \omega_{\mathbf{a}} \beta_{\mathbf{a}}(\mathbf{x})}, \qquad \mathbf{x} \in I_{\mathcal{A}}.$$

is called a **toric surface patch** (or toric Bézier patch, toric patch) defined in $\mathbb{R}^m$.

Why toric? It is the projection of toric variety. The mathematical theory is from **toric ideals of Combinatorics** and **toric varieties of Algebraic Geometry**.

Special cases

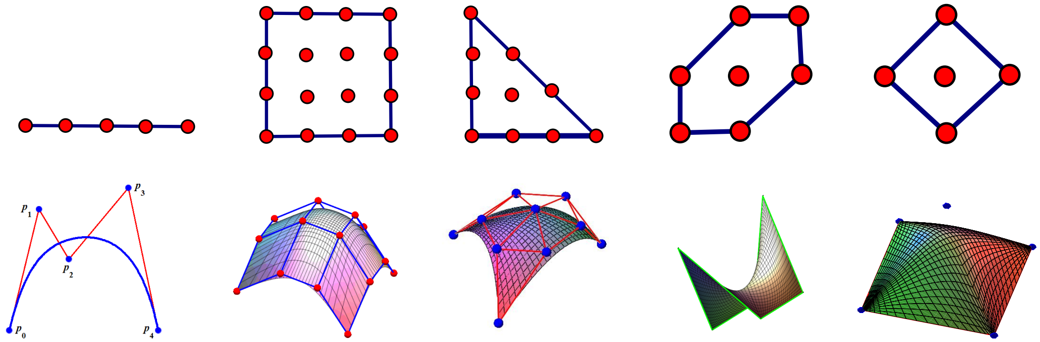

Example: Lattice heptahedron and 3D toric volume

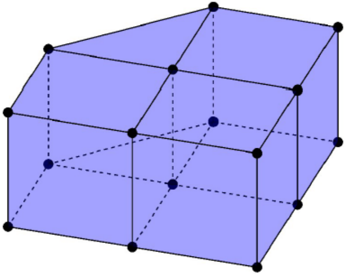

$I_{\mathcal{A}}, d = 3$

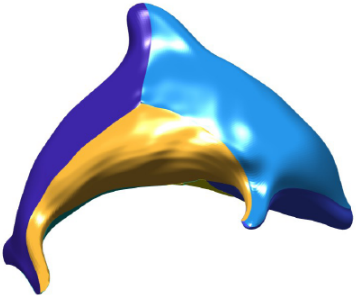

toric volume, $m = 3$

Outlines

Geometric meaning of weights

A famous geometric meaning of weights is that the large weight pulls the surface patch towards the corresponding control point.

Geometric meaning of weights

A famous geometric meaning of weights is that the large weight pulls the surface patch towards the corresponding control point.

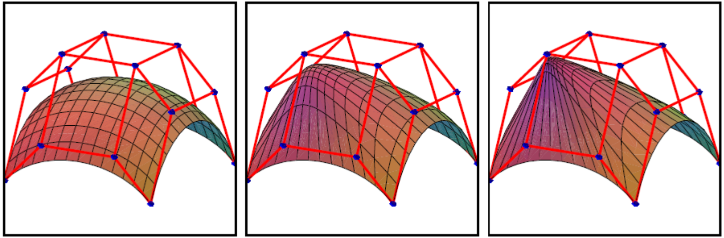

Geometric meaning of weights

For given weights w, set $w_\lambda(t) = \{t^{\lambda(\mathbf{a})} w_{\mathbf{a}} \mid \mathbf{a} \in \mathcal{A}\}$ for $t > 0$. Let

$$\mathcal{B}_{\mathcal{A},\omega_\lambda(t),\mathcal{P}}(u,v;t) = \frac{\sum_{\mathbf{a}\in\mathcal{A}} \mathbf{P}_{\mathbf{a}} t^{\lambda(\mathbf{a})} \omega_{\mathbf{a}} \beta_{\mathbf{a}}(u,v)}{\sum_{\mathbf{a}\in\mathcal{A}} t^{\lambda(\mathbf{a})} \omega_{\mathbf{a}} \beta_{\mathbf{a}}(u,v)}, \quad (u,v) \in I_{\mathcal{A}}.$$

and the patch $\mathcal{B}_{\mathcal{A},w_\lambda(t),\mathcal{P}}$ parameterized by $\mathcal{B}_{\mathcal{A},w_\lambda(t),\mathcal{P}}(u,v;t)$.

Geometric meaning of weights

For given weights w, set $w_\lambda(t) = \{t^{\lambda(\mathbf{a})} w_{\mathbf{a}} \mid \mathbf{a} \in \mathcal{A}\}$ for $t > 0$. Let

$$\mathcal{B}_{\mathcal{A},\omega_\lambda(t),\mathcal{P}}(u,v;t) = \frac{\sum_{\mathbf{a}\in\mathcal{A}} \mathbf{P}_{\mathbf{a}} t^{\lambda(\mathbf{a})} \omega_{\mathbf{a}} \beta_{\mathbf{a}}(u,v)}{\sum_{\mathbf{a}\in\mathcal{A}} t^{\lambda(\mathbf{a})} \omega_{\mathbf{a}} \beta_{\mathbf{a}}(u,v)}, \quad (u,v) \in I_{\mathcal{A}}.$$

and the patch $\mathcal{B}_{\mathcal{A},w_\lambda(t),\mathcal{P}}$ parameterized by $\mathcal{B}_{\mathcal{A},w_\lambda(t),\mathcal{P}}(u,v;t)$.

Theorem (Toric degeneration. García-Puente, Sottile and Zhu, 2011)

For a toric surface $\mathcal{B}_{\mathcal{A},w_\lambda,\mathcal{P}}$,

$$\lim_{t\to\infty} \mathcal{B}_{\mathcal{A},\omega_\lambda(t),\mathcal{P}} = \mathcal{B}_{\mathcal{A},\omega,\mathcal{P}}(\mathcal{S}_\lambda),$$

where $\mathcal{B}_{\mathcal{A},\omega,\mathcal{P}}(\mathcal{S}_\lambda)$ is called the regular control surface of $\mathcal{B}_{\mathcal{A},w_\lambda,\mathcal{P}}$ induced by regular decomposition $\mathcal{S}_\lambda$.

Example: quartic rational Bézier curve

$\mathcal{A} = \{0, 1, 2, 3, 4\}$, $\lambda(\mathcal{A}) = \{1, 2, 3, 2, 1\}$
$\mathcal{S}_\lambda = \{\{0, 1, 2\}, \{2, 3, 4\}\}$

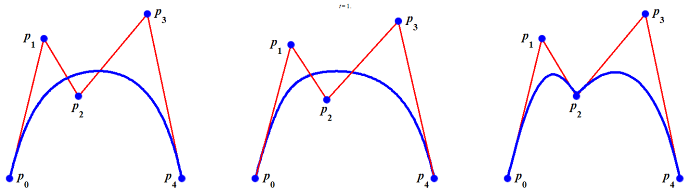

(a) Quartic rational Bézier curve $\mathcal{B}_{\mathcal{A},\omega,\mathcal{P}}$.

(b) $\lim_{t\to\infty} \mathcal{B}_{\mathcal{A},\omega_\lambda(t),\mathcal{P}}$.

(c) Regular control curve $\mathcal{B}_{\mathcal{A},\omega,\mathcal{P}}(\mathcal{S}_\lambda)$.

Example: quartic rational Bézier curve

$\mathcal{A} = \{0, 1, 2, 3, 4\}$, $\lambda(\mathcal{A}) = \{1, 2, 3, 1, 2\}$
$\mathcal{S}_\lambda = \{\{0, 1, 2\}, \{2, 4\}\}$

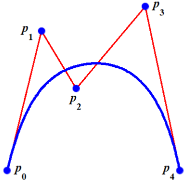

(d) Quartic rational Bézier curve $\mathcal{B}_{\mathcal{A},\omega,\mathcal{P}}$.

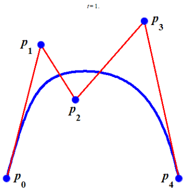

(e) $\lim_{t\to\infty} \mathcal{B}_{\mathcal{A},\omega_\lambda(t),\mathcal{P}}$.

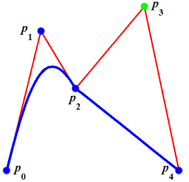

(f) Regular control curve $\mathcal{B}_{\mathcal{A},\omega,\mathcal{P}}(\mathcal{S}_\lambda)$.

Example: trapezoidal toric patch

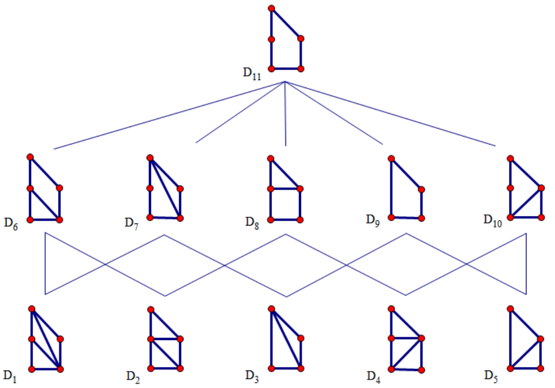

Example: trapezoidal toric patch

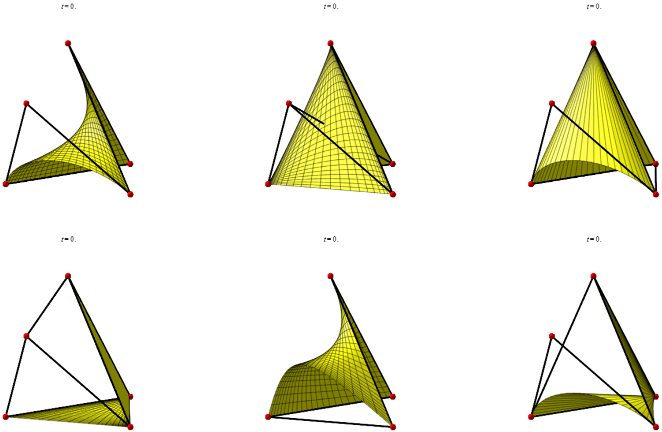

Example: trapezoidal toric patch

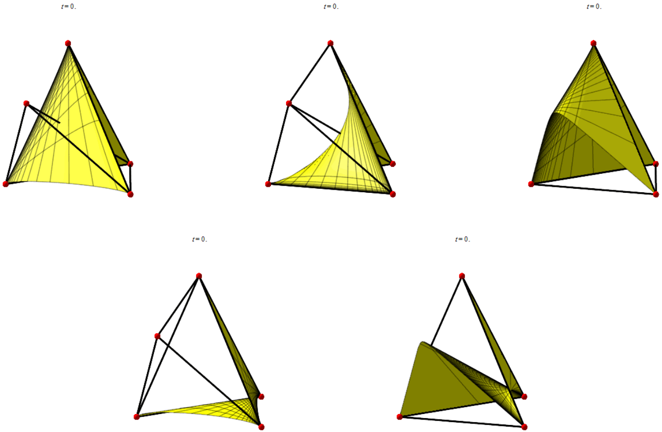

Example: bi-quadric Bézier patch

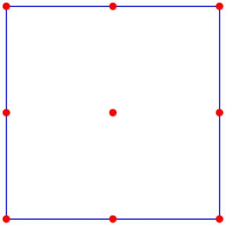

$\mathcal{A}_{2,2}$

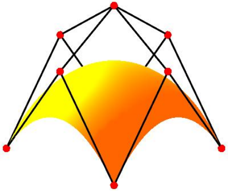

$\mathcal{B}_{\mathcal{A}_{2,2},\omega,\mathcal{P}}$

Example:bi-quadric Bézier patch

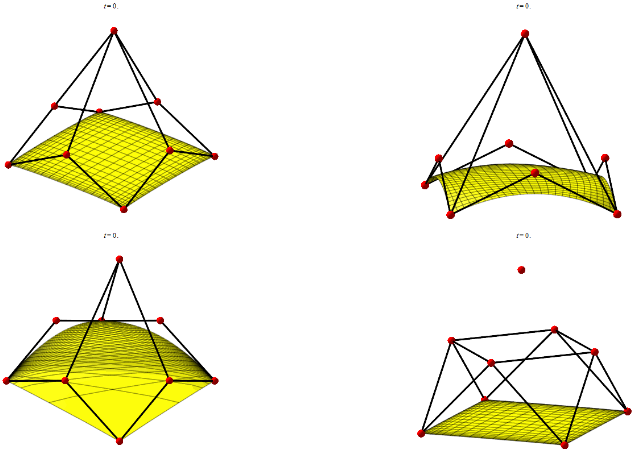

Application to curve and surface deformation

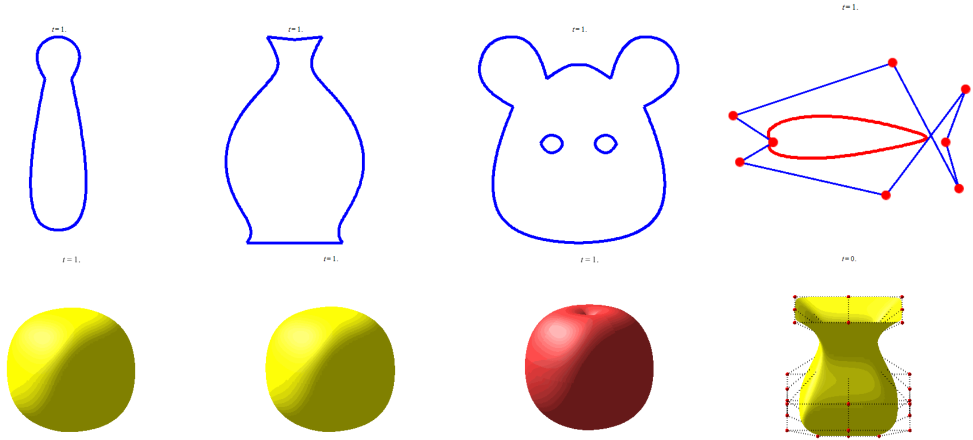

Outlines

Injectivity of 2D toric surfaces

Theorem (Sottile & Zhu, 2011)

Suppose $\mathcal{A} \subset \mathbb{Z}^2$ and $\mathcal{P} \subset \mathbb{R}^2$. The map $\mathcal{B}_{\mathcal{A},\omega,\mathcal{P}} : I_{\mathcal{A}} \mapsto \mathbb{R}^2$ is injective for all $\omega \in \mathbb{R}^{\mathcal{A}}_{>}$ if and only if $\mathcal{A}$ and $\mathcal{P}$ are compatible.

Injectivity of 2D toric surfaces

Theorem (Sottile & Zhu, 2011)

Suppose $\mathcal{A} \subset \mathbb{Z}^2$ and $\mathcal{P} \subset \mathbb{R}^2$. The map $\mathcal{B}_{\mathcal{A},\omega,\mathcal{P}} : I_{\mathcal{A}} \mapsto \mathbb{R}^2$ is injective for all $\omega \in \mathbb{R}^{\mathcal{A}}_{>}$ if and only if $\mathcal{A}$ and $\mathcal{P}$ are compatible.

Theorem (Pick's Theorem, G. Pick, 1899)

Given a simple polygon whose vertex coordinates are all integral points, its area S, the number of internal lattice points k, and the number of lattice points m on the boundary of the polygon satisfy: $S = k + \frac{m}{2} - 1$.

Definition (Farey Sequence, J. Farey, 1816)

The Farey sequence F_k for any positive integer k is the set of irreducible rational numbers $\frac{a}{b}$ with $0 \le a \le b \le k$ and $gcd(a, b) = 1$ arranged in increasing order.

Improved checking algorithm

Theorem (Yu, Ji & Zhu, 2020)

Suppose $\mathcal{A} = \mathcal{A}_{k,l} = \{(i,j) \in \mathbb{Z}^2 | 0 \leqslant i \leqslant k, 0 \leqslant j \leqslant l\}$*, where* k, l *are positive integers and* $n = k \times l$ *points. Then complexity of improved algorithm is* $O(k^3 l)$ *for* $\forall k, l \in \mathbb{Z}$*, or* $O(n^2)$ *for* $k = cl$ *or* $k = l$*, where* $c > 0$ *is a positive constant independent of* n*.*

Improved checking algorithm

Theorem (Yu, Ji & Zhu, 2020)

Suppose $\mathcal{A} = \mathcal{A}_{k,l} = \{(i,j) \in \mathbb{Z}^2 | 0 \leqslant i \leqslant k, 0 \leqslant j \leqslant l\}$*, where* k, l *are positive integers and* $n = k \times l$ *points. Then complexity of improved algorithm is* $O(k^3 l)$ *for* $\forall k, l \in \mathbb{Z}$*, or* $O(n^2)$ *for* $k = cl$ *or* $k = l$*, where* $c > 0$ *is a positive constant independent of* n*.*

Theorem (Yu, Ji & Zhu, 2020)

For general lattice set $\mathcal{A} \subset \mathbb{Z}^2$ *with* $\#(\mathcal{A}) = n$*, the complexity of improved algorithm is* $O(n^2)$*.*

Example: tensor-product Bézier surface

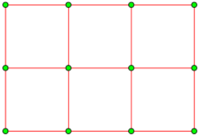

(a) lattice points

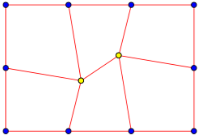

(b) control points

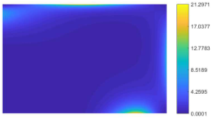

(c) Jacobian for Figure 6(b)

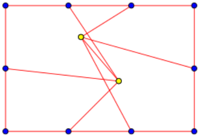

(d) control points

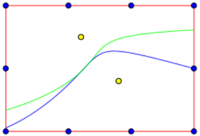

(e) isoparametric curves

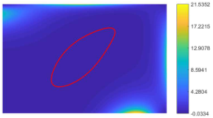

(f) Jacobian for Figure

Example: tensor-product Bézier surface

n	10^2	20^2	30^2	40^2
Improved algorithm	**0.0288**	**0.2306**	**0.8244**	**1.9381**
Algorithm in [Sottile & Zhu, 2011]	2.5731	167.31	2044.69	$*$

Table: Computation times for $\mathcal{A}_{k,k}$

Example: triangular Bézier surface

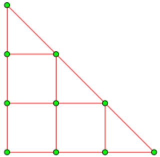

(a) lattice points

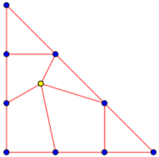

(b) control points

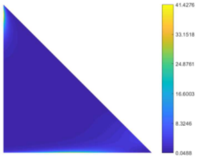

(c) Jacobian for Figure 7(b)

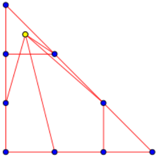

(d) control points

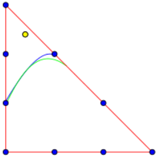

(e) isoparametric curves

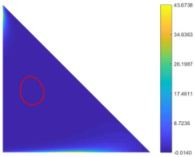

(f) Jacobian for Figure

Example: triangular Bézier surface

n	$\binom{10+2}{2}$	$\binom{20+2}{2}$	$\binom{30+2}{2}$	$\binom{40+2}{2}$
Improved algorithm	**0.0094**	**0.0759**	**0.2775**	**5.915**
Algorithm in [Sottile & Zhu, 2011]	0.4144	24.1250	273.67	$*$

Table: Computation times for $\mathcal{A}_k$

Example: hexagonal surface

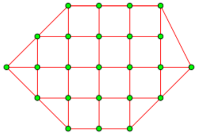

(a) lattice points

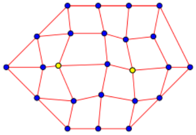

(b) control points

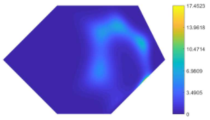

(c) Jacobian for Figure 8(b)

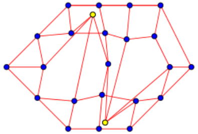

(d) control points

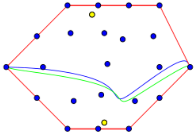

(e) isoparametric curves

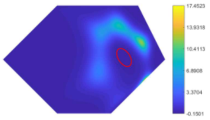

(f) Jacobian for Figure 8(d)

Injectivity of 3D toric volumes

Theorem (Yu, Ji, Li & Zhu, 2021)

Suppose $\mathcal{A} \subset \mathbb{Z}^3$ and $\mathcal{P} \subset \mathbb{R}^3$. The map $\mathcal{B}_{\mathcal{A},\omega,\mathcal{P}} : I_{\mathcal{A}} \to \mathbb{R}^3$ is injective for arbitrary positive weights $\omega = \{\omega_{\mathbf{a}} > 0 | \mathbf{a} \in \mathcal{A}\}$ if and only if the lattice points set $\mathcal{A}$ and control points set $\mathcal{P}$ are compatible.

Injectivity of 3D toric volumes

Theorem (Yu, Ji, Li & Zhu, 2021)

Suppose $\mathcal{A} \subset \mathbb{Z}^3$ and $\mathcal{P} \subset \mathbb{R}^3$. The map $\mathcal{B}_{\mathcal{A},\omega,\mathcal{P}} : I_{\mathcal{A}} \to \mathbb{R}^3$ is injective for arbitrary positive weights $\omega = \{\omega_{\mathbf{a}} > 0 | \mathbf{a} \in \mathcal{A}\}$ if and only if the lattice points set $\mathcal{A}$ and control points set $\mathcal{P}$ are compatible.

Theorem (Reznick, 2006)

The clean tetrahedron T is also empty if and only if $T \sim T_{0,0,1}$ or $T \sim T_{1,t,k}$, where $gcd(t,k) = 1$ and $1 \leq t \leq k-1$.

Examples: lattice pentahedron

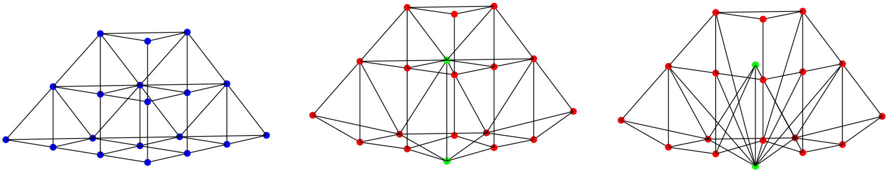

(a) Lattice points set $\mathcal{A}$ (b) Control points set $\mathcal{P}_1$ (c) Control points set $\mathcal{P}_2$

Examples: toric pentahedron

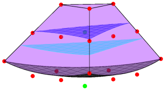

(d) Toric volume $\mathcal{B}_{\mathcal{A},\omega_1,\mathcal{P}_1}$

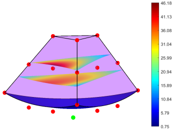

(e) Jacobian for $\mathcal{B}_{\mathcal{A},\omega_1,\mathcal{P}_1}$

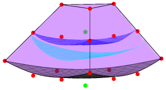

(f) Toric volume $\mathcal{B}_{\mathcal{A},\omega_2,\mathcal{P}_1}$

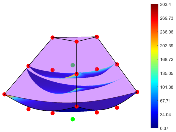

(g) Jacobian for $\mathcal{B}_{\mathcal{A},\omega_2,\mathcal{P}_1}$

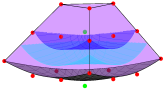

(h) Toric volume $\mathcal{B}_{\mathcal{A},\omega_3,\mathcal{P}_1}$

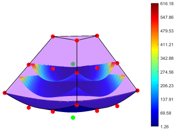

(i) Jacobian for $\mathcal{B}_{\mathcal{A},\omega_3,\mathcal{P}_1}$

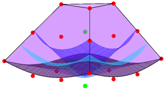

(j) Toric volume $\mathcal{B}_{\mathcal{A},\omega_3,\mathcal{P}_2}$

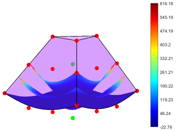

(k) Jacobian for $\mathcal{B}_{\mathcal{A},\omega_3,\mathcal{P}_2}$

Example: polyhedron derived from cutting a corner from the cube $I_{\mathcal{A}_{k,k,k}}$

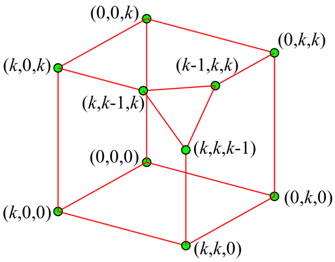

Comparison of the amounts of lattice tetrahedrons checked in above polyhedron

k	2	3	4	5
Original algorithm	**14950**	**595665**	**9381251**	**86567815**
Improved algorithm	**7875**	**277323**	**4130122**	**34212398**
Percentage	0.53	0.47	0.44	0.40

Outlines

Toric surface patches of depth d

Definition

Given a lattice set $\mathcal{A} \subset \mathbb{Z}^2$, a positive integer d, weights $\omega = \{\omega_\gamma \geq 0\}_{\gamma \in \mathcal{A}^d}$ and control points $\mathcal{P} = \{\mathbf{P}_\gamma\}_{\gamma \in \mathcal{A}^d} \in \mathbb{R}^3$, the **toric surface patch of depth d** is defined as

$$\mathcal{B}_{\mathcal{A}^d,\omega,\mathcal{P}}(u,v) = \frac{\sum_{\gamma \in \mathcal{A}^d} \omega_\gamma \mathbf{P}_\gamma B_\gamma^d(u,v)}{\sum_{\gamma \in \mathcal{A}^d} \omega_\gamma B_\gamma^d(u,v)} \qquad (u,v) \in NP(\mathcal{A}). \tag{2.1}$$

where $NP(\mathcal{A})$ is the Newton polygon of $\mathcal{A}$, $\mathcal{A}^d$ is the d summands Minkowski sum of $\mathcal{A}$, basis functions $\{B_\gamma^d(u,v)\}_{\gamma \in \mathcal{A}^d}$ are generated by the d discrete convolution of toric Bernstein basis functions $\{\beta_{\mathbf{a}}(u,v)\}_{\boldsymbol{a} \in \mathcal{A}}$.

de Casteljau algorithm

Theorem (Li, Ji & Zhu, 2021)

For $(u^*, v^*) \in NP(I)$, *the point* $\mathcal{B}_{\mathcal{A}^d,\omega,\mathcal{P}}(u^*, v^*)$ *on the surface* $\mathcal{B}_{\mathcal{A}^d,\omega,\mathcal{P}}(u, v)$ *can be computed recursively by*

$$\begin{cases} \omega_{\boldsymbol{\gamma}^0}(u^*, v^*) \equiv \omega_{\boldsymbol{\gamma}^0} = \omega_{\boldsymbol{\gamma}}, & \boldsymbol{\gamma} \in \mathcal{A}^d, \\ \omega^l_{\boldsymbol{\gamma}}(u^*, v^*) = \sum_{\boldsymbol{a}\in\mathcal{A}} \beta_{\boldsymbol{a}}(u^*, v^*)\omega^{l-1}_{\boldsymbol{\gamma}+\boldsymbol{a}}(u^*, v^*), & \boldsymbol{\gamma} \in \mathcal{A}^{d-l}. \end{cases}$$

$$\begin{cases} \mathbf{P}^0_{\boldsymbol{\gamma}}(u^*, v^*) \equiv \mathbf{P}^0_{\boldsymbol{\gamma}} = \mathbf{P}_{\boldsymbol{\gamma}}, & \boldsymbol{\gamma} \in \mathcal{A}^d, \\ \mathbf{P}^l_{\boldsymbol{\gamma}}(u^*, v^*) = \dfrac{\sum_{\boldsymbol{a}\in\mathcal{A}} \beta_{\boldsymbol{a}}(u^*, v^*)\omega^{l-1}_{\boldsymbol{\gamma}+\boldsymbol{a}}(u^*, v^*)\mathbf{P}^{l-1}_{\boldsymbol{\gamma}+\boldsymbol{a}}(u^*, v^*)}{\omega^l_{\boldsymbol{\gamma}}(u^*, v^*)}, & \boldsymbol{\gamma} \in \mathcal{A}^{d-l}. \end{cases}$$

where $l = 1, \cdots, d$.

Example: pentagonal patch

$$d = 2, u^* = 1, v^* = 1$$

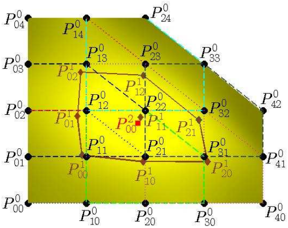

(l) Top view.

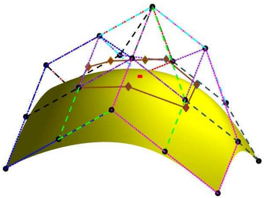

(m) Side view.

Example: pentagonal patch

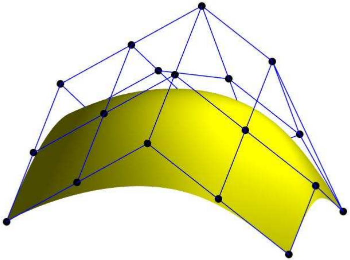

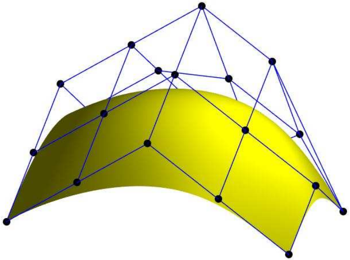

Outlines

1. **Background**
2. **Toric surface patches**
   - Definition
   - Geometric meaning of weights
   - Injectivity
   - De Casteljau algorithm
   - Degree elevation
   - Subdivision
3. **Generalized Bézier surfaces**
4. **Application to IGA**

Degree elevation

Theorem (Li, Ji & Zhu, 2021)

For any positive integer q*, toric surface* $\mathcal{B}_{\mathcal{A}^d,\omega,\mathcal{P}}(u,v)$ *of depth* d *can be represented in* $\mathcal{B}_{\mathcal{A}^{d+q},\widetilde{\omega},\widetilde{\mathcal{P}}}(u,v)$ *of depth* $d+q$*, where* $\widetilde{\omega} = \{\omega_{\boldsymbol{\gamma}}^{d+q}\}_{\boldsymbol{\gamma}\in\mathcal{A}^{d+q}}, \widetilde{\mathcal{P}} = \{\mathbf{P}_{\boldsymbol{\gamma}}^{d+q}\}_{\boldsymbol{\gamma}\in\mathcal{A}^{d+q}}$

$$\mathbf{P}_{\boldsymbol{\gamma}}^{d+q} = \left(\sum_{\boldsymbol{\eta}\in\mathcal{A}^q} \frac{c_{\boldsymbol{\eta}}^q c_{\boldsymbol{\gamma}-\boldsymbol{\eta}}^d}{c_{\boldsymbol{\gamma}}^{d+q}} \omega_{\boldsymbol{\gamma}-\boldsymbol{\eta}}^d \mathbf{P}_{\boldsymbol{\gamma}-\boldsymbol{\eta}}^d\right) / \omega_{\boldsymbol{\gamma}}^{d+q}, \tag{2.4}$$

$$\omega_{\boldsymbol{\gamma}}^{d+q} = \sum_{\boldsymbol{\eta}\in\mathcal{A}^q} \frac{c_{\boldsymbol{\eta}}^q c_{\boldsymbol{\gamma}-\boldsymbol{\eta}}^d}{c_{\boldsymbol{\gamma}}^{d+q}} \omega_{\boldsymbol{\gamma}-\boldsymbol{\eta}}^d. \tag{2.5}$$

Example: pentagonal and hexagonal toric surfaces

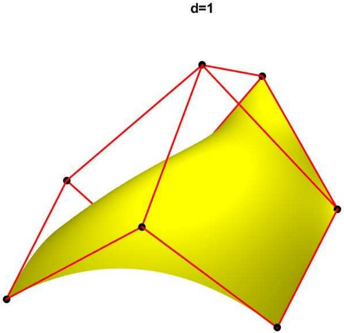

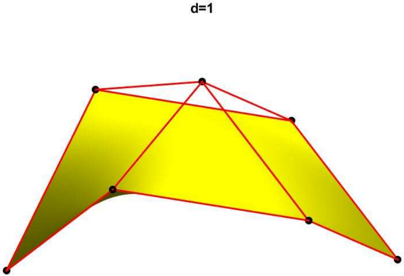

Outlines

Subdivision (decomposition)

Theorem (Ji, Li, Yu & Zhu, 2022)

The N-sided toric surface patch $\mathcal{B}_{\mathcal{A},\omega,\mathcal{P}}(u,v)$ can be subdivided into N rational tensor product Bézier surface patches $\widetilde{\mathcal{S}}_k(s_k,t_k), k=1,2,\cdots,N$, i.e.,

$$\mathcal{B}_{\mathcal{A},\omega,\mathcal{P}} = \bigcup_{k=1}^{N} \widetilde{\mathcal{S}}_k, \tag{2.6}$$

where $\mathcal{B}_{\mathcal{A},\omega,\mathcal{P}}$ is the image set of toric mapping, and $\widetilde{\mathcal{S}}_k$ is the image set of the resulting rational tensor product Bézier mapping.

Example: pentagonal and hexagonal toric surfaces

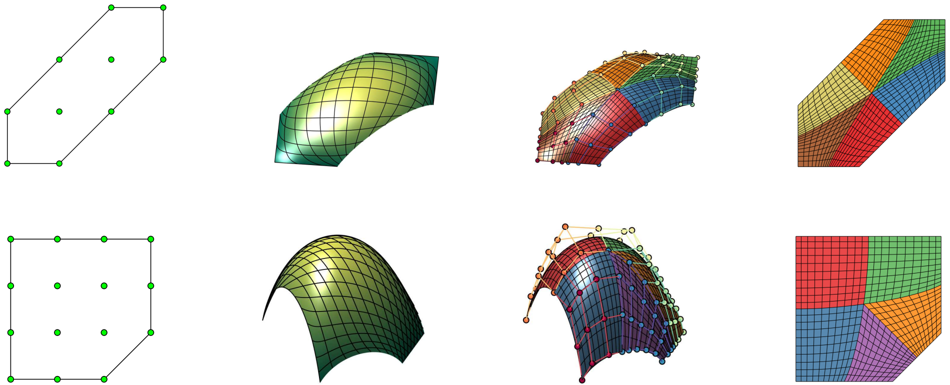

(r) $I_{\mathcal{A}}$ (s) Original patch (t) Subdivision result (u) Vertical view

Outlines

Generalized Bézier surface

Definition (Várady, Salvi, Karikó, 2016)

Given an n-sided convex polygonal domain $\mathcal{P}$, denote the Wachspress barycentric coordinates of $\mathcal{P}$ by $\lambda_i, i = 1, \cdots, n$. Let θ_i be the angles of $\mathcal{P}$. Given the control points $\mathbf{C}_{j,k}^{d,i}, j = 0, \cdots, d, k = 0, \cdots, l-1$, where d is the degree of surface, $l = \lceil \frac{d}{2} \rceil$ is the number of control point layers. The **generalized Bézier (GB) surface** is the image of the mapping $\mathbf{S}^d : \mathcal{P} \to \mathbb{R}^3$, $\forall (u,v) \in \mathcal{P}$,

$$\mathbf{S}^d(u,v) = \sum_{i=1}^{n} \sum_{j=0}^{d} \sum_{k=0}^{l-1} \mu_{j,k}^{i} \mathbf{C}_{j,k}^{d,i} B_{j,k}^{d,d}(s_i(u,v), h_i(u,v)) + \mathbf{C}_0^d B_0^d(u,v), \tag{3.1}$$

where $s_i = \frac{\sin(\theta_i) g_{i-1}^{\perp}}{\sin(\theta_i) g_{i-1}^{\perp} + \sin(\theta_{i-1}) g_{i+1}^{\perp}}$, $h_i = 1 - \lambda_{i-1} - \lambda_i$ are the local parameters,

Generalized Bézier surface

Definition (cont.)

$$B^{d,d}_{j,k}(s_i,h_i) = B^d_j(s_i)B^d_k(h_i) = \binom{d}{j}(1-s_i)^{d-j}s_i^j\binom{d}{k}(1-h_i)^{d-k}h_i^k$$

are Bernstein basis functions of (s_i,h_i), $\mathbf{C}^d_0 = \frac{1}{n}\sum_{i=1}^{n}\mathbf{C}^{d,i}_{l,l-1}$ is the central point and its corresponding blending function

$$B^d_0(u,v) = 1 - \sum_{i=1}^{n}\sum_{j=0}^{d}\sum_{k=0}^{l-1}\mu^i_{j,k}B^{d,d}_{j,k}(s_i(u,v),h_i(u,v)), \quad (3.2)$$

and $\mu^i_{j,k}$ are weights.

Example: pentagonal GB surface $(d = 4, n = 5)$

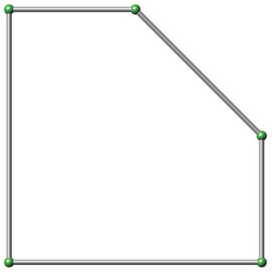

(v) Pentagonal parametric domain

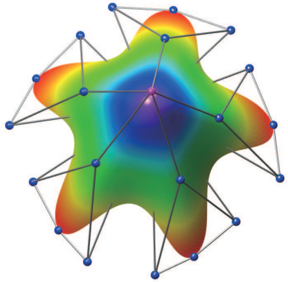

(w) Pentagonal GB surface

Example: complex models (Várady et al. 2016)

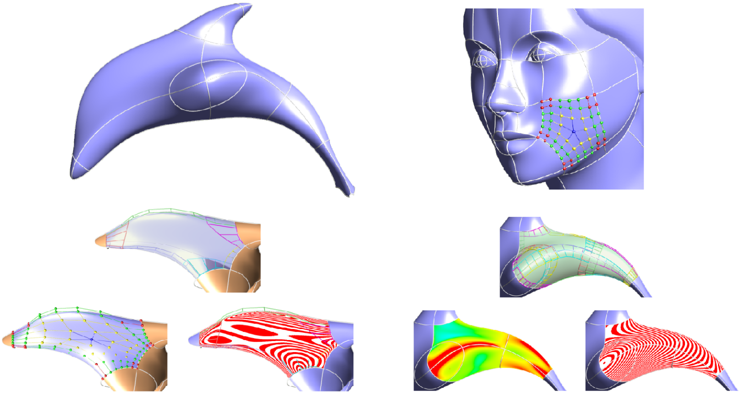

Outlines

1 Background

2 Toric surface patches

3 Generalized Bézier surfaces
- Definition
- Degree elevation
- Knot insertion

4 Application to IGA

Improved Degree elevation

Theorem (Wang, Ji, Zhu, 2022)

The GB surface of degree d $\mathbf{S}^d(u,v) = \sum_{i=1}^{n}\sum_{j=0}^{d}\sum_{k=0}^{l-1}\tilde{\mathbf{C}}_{j,k}^{d,i}B_{j,k}^{d,d}(s_i(u,v),h_i(u,v)) + \mathbf{C}_0^d B_0^d(u,v)$ *can be represented as a GB surface of degree* $d+1$ *as*

$$\mathbf{S}^{d+1}(u,v) = \sum_{i=1}^{n}\sum_{j=0}^{d+1}\sum_{k=0}^{l}\tilde{\mathbf{C}}_{j,k}^{d+1,i}B_{j,k}^{d+1,d+1}(s_i(u,v),h_i(u,v)) + \mathbf{C}_0^d B_0^d(u,v), \quad (3.3)$$

where $\tilde{\mathbf{C}}_{j,k}^{d,i} = \mu_{j,k}^{i}\mathbf{C}_{j,k}^{d,i}$, *and the control points* $\tilde{\mathbf{C}}_{j,k}^{d+1,i}$ *satisfy*

$$\tilde{\mathbf{C}}_{j,k}^{d+1,i} = \eta_j\upsilon_k\tilde{\mathbf{C}}_{j-1,k-1}^{d,i} + (1-\eta_j)\upsilon_k\tilde{\mathbf{C}}_{j,k-1}^{d,i} + \eta_j(1-\upsilon_k)\tilde{\mathbf{C}}_{j-1,k}^{d,i} + (1-\eta_j)(1-\upsilon_k)\tilde{\mathbf{C}}_{j,k}^{d,i}. \quad (3.4)$$

Example: degree elevation for hexagonal and heptagonal GB surfaces

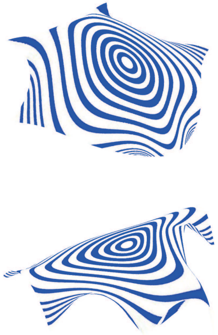

(aa) Initial surface

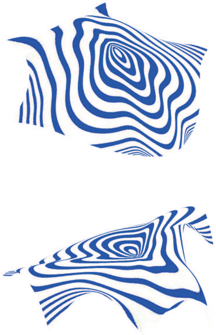

(ab) After degree elevation (Várady et al. 2016)

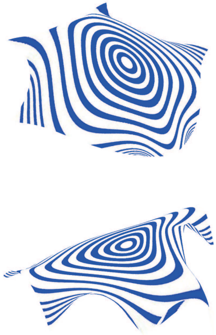

(ac) After degree elevation (ours)

Outlines

Knot insertion

Theorem (Wang, Ji, Zhu, 2022)

Assume that $\{\underbrace{0,\cdots,0}_{(d+1)-times},\underbrace{1,\cdots,1}_{(d+1)-times}\}\subset\bar{\mathbf{U}}$ *and* $\{\underbrace{0,\cdots,0}_{(d+1)-times},\underbrace{1,\cdots,1}_{(d+1)-times}\}\subset\bar{\mathbf{V}}$, *then the GB surface* $\mathbf{S}^d(u,v)=\sum_{i=1}^{n}\sum_{j=0}^{d}\sum_{k=0}^{l-1}\widetilde{\mathbf{C}}_{j,k}^{d,i}N_{j,k}^{d,d}(s_i(u,v),h_i(u,v))+\mathbf{C}_0^dB_0^d(u,v)$ *can be represented as*

$$\bar{\mathbf{S}}^d(u,v)=\sum_{i=1}^{n}\sum_{j=0}^{m_u+d}\sum_{k=0}^{m_v+l-1}\bar{\mathbf{C}}_{j,k}^{d,i}\bar{N}_{j,k}^{d,d}(s_i(u,v),h_i(u,v))+\mathbf{C}_0^dB_0^d(u,v), \tag{3.5}$$

where $\bar{N}_{j,k}^{d,d}$ *are B-spline basis functions of spline space* $\mathcal{S}_{\bar{\mathbf{U}},\bar{\mathbf{V}}}^{d,d}$, *and the collection of control points* $\mathbf{P}^{d,i}=[\widetilde{\mathbf{C}}_{j,k}^{d,i}]_{(d+1)\times l}$ *and* $\bar{\mathbf{P}}^{d,i}=[\bar{\mathbf{C}}_{j,k}^{d,i}]_{(m_u+d+1)\times(m_v+l)}$.

Example: knot insertion for hexagonal and heptagonal GB surfaces

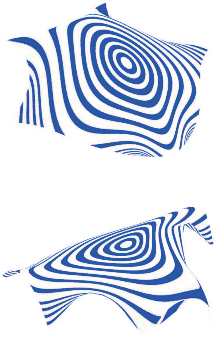

(af) Initial surface

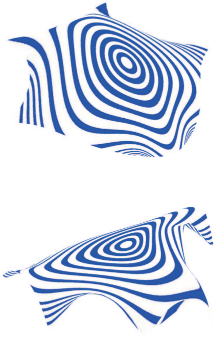

(ag) After knot insertion

Outlines

Domain parameterization in IGA

- Constructing **analysis-suitable parameterization of computational domain** is a crucial step in IGA

Domain parameterization in IGA

- Constructing **analysis-suitable parameterization of computational domain** is a crucial step in IGA
- Prerequisite: **injectivity**

Domain parameterization in IGA

- Constructing **analysis-suitable parameterization of computational domain** is a crucial step in IGA
- Prerequisite: **injectivity**
- Refinement methods: **h-refinement, p-refinement, k-refinement**

Domain parameterization in IGA

- Constructing **analysis-suitable parameterization of computational domain** is a crucial step in IGA
- Prerequisite: **injectivity**
- Refinement methods: **h-refinement, p-refinement, k-refinement**
- Parameterization methods: Bézier/B-splines/NURBS, T-splines, unstructured splines, multi-patch methods, TCB splines, $\cdots$

Domain parameterization in IGA

- Constructing **analysis-suitable parameterization of computational domain** is a crucial step in IGA
- Prerequisite: **injectivity**
- Refinement methods: **h-refinement, p-refinement, k-refinement**
- Parameterization methods: Bézier/B-splines/NURBS, T-splines, unstructured splines, multi-patch methods, TCB splines, $\cdots$
- Proposed multi-sided parameterization methods: **injective preserving toric parameterization and GB parametrization** with h-, p-, k-refinements

Outlines

Injective preserving toric parameterization with p-refinement for Possion's equation

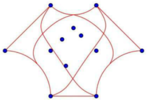

(a) Meshes of $d = 1$.

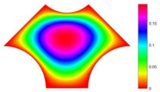

(b) Colormap of numerical solution of $d = 1$.

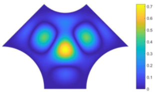

(c) Error colormap corresponding to $d = 1$.

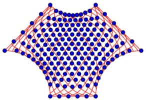

(d) Meshes of $d = 5$.

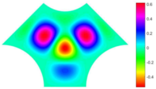

(e) Colormap of numerical solution of $d = 5$.

(f) Error colormap corresponding to $d = 5$.

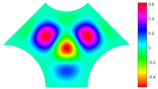

(g) Colormap of exact solution.

Comparison

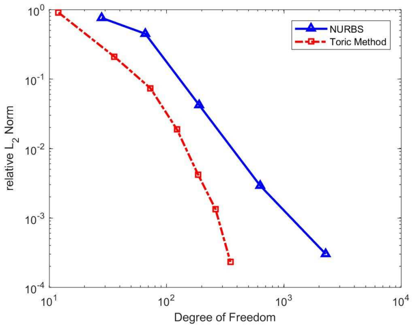

Figure: Relative L_2 error norm history during p-refinement.

h-Refinement strategy of toric parameterization

h-Refinement method for toric parameterization of planar multi-sided computational domain in isogeometric analysis

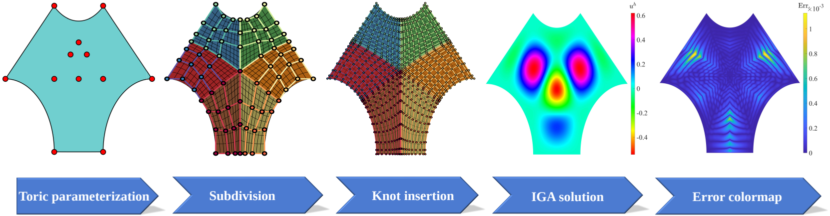

Toric parameterization with p-, h-refinements for Possion’s equation

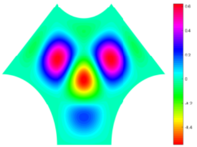

(a) Colormap of exact solution

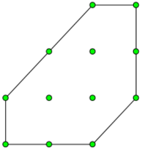

(b) Hexagonal parametric domain and lattice points

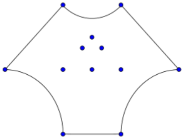

(c) Toric parameterization and control points

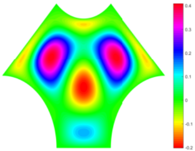

(d) Colormap of toric DEM solution (DOF=36)

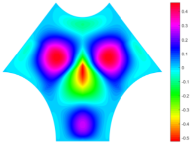

(b) Colormap of the solution on the coarsest mesh (DOF=73)

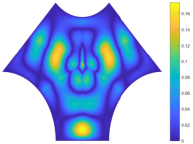

(c) Error colormap on the coarsest mesh (DOF=73)

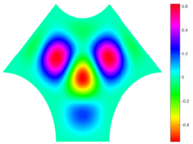

(d) Colormap of the solution on the refined mesh (DOF=661)

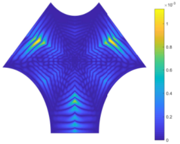

(e) Error colormap on the refined mesh (DOF=661)

Comparison

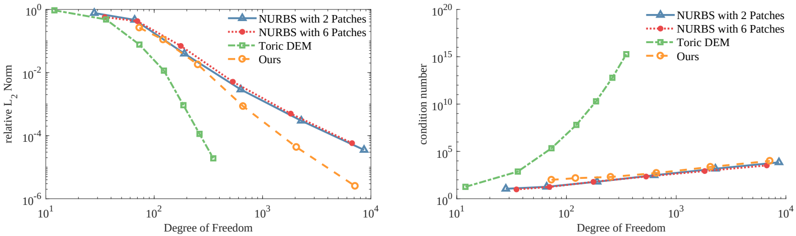

(a) Relative L_2 norm error

(b) Condition number of the stiffness matrix

NURBS and toric parameterizations for linear elasticity problem

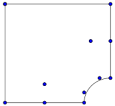

(a) control points and Bézier patches w.r.t. C^1 parameterization

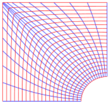

(b) C^1 parameterization in [5]

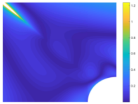

(c) Colormap of absolute error of stress in x-direction w.r.t. (b)

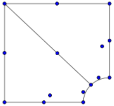

(d) NURBS with two Bézier patches and control points

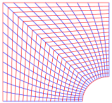

(e) NURBS paraterization with two Bézier patches

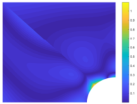

(f) Colormap of absolute error of stress in x-direction w.r.t. (e)

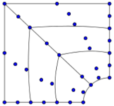

(g) NURBS with six Bézier patches and control points

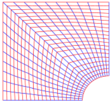

(h) NURBS paraterization with six Bézier patches

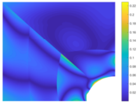

(i) Colormap of absolute error of stress in x-direction w.r.t. (h)

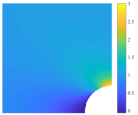

(a) Colormap of exact solution of stress in x-direction

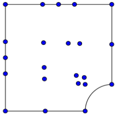

(b) Pentagonal toric parameterization

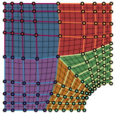

(c) Subdivision result

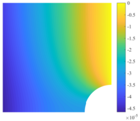

(d) Colormap of the IGA solution of displacement in x-direction

(e) Colormap of the IGA solution of stress in x-direction

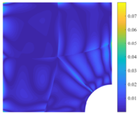

(f) Colormap of absolute error of stress in x-direction w.r.t. (c)

Comparison

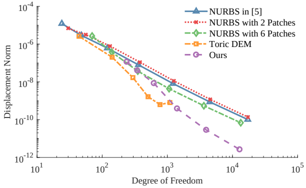

(c) Displacement norm error

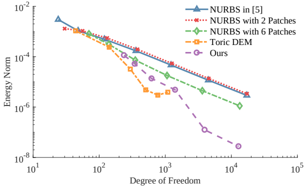

(d) Energy norm error

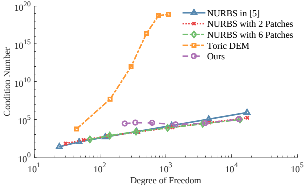

(e) Condition number of the stiffness matrix

Outlines

GB, toric and NURBS parameterizations for Poisson's equation

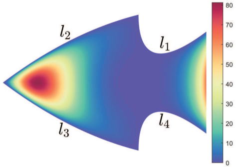

(f) Exact solution

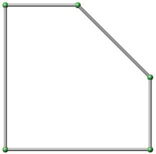

(g) Parametric domain of GB surface

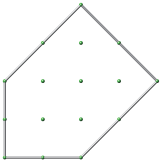

(h) Lattice points of toric surface

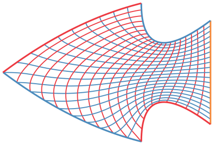

(i) GB parameterization

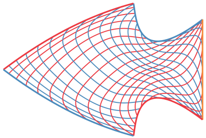

(j) Toric parameterization

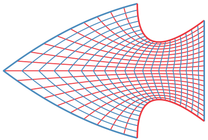

(k) NURBS parameterization

GB, toric and NURBS parameterizations for Poisson's equation

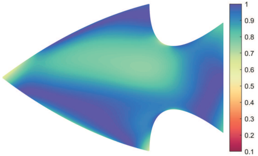

(a) J_s on GB surface

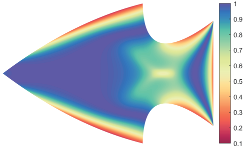

(b) J_s on toric surface

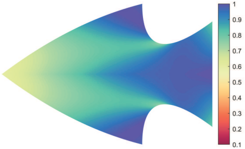

(c) J_s on NURBS surface

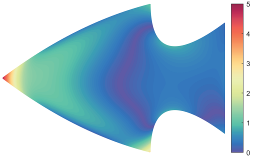

(d) S_a on GB surface

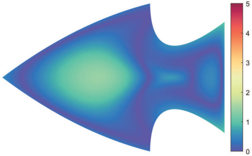

(e) S_a on toric surface

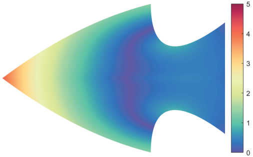

(f) S_a on NURBS surface

GB, toric and NURBS parameterizations for Poisson's equation

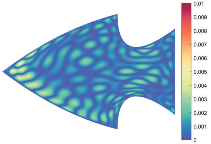

(a) Error on GB surface by p-refinement (DOFs=441)

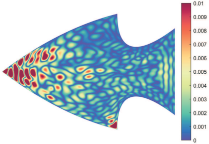

(b) Error on GB surface by h-refinement (DOFs=541)

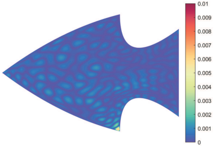

(c) Error on GB surface by k-refinement (DOFs=541)

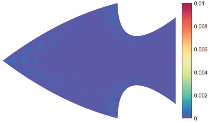

(d) Error on toric surface (DOFs=391)

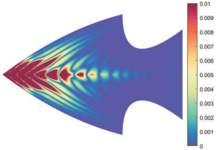

(e) Error on NURBS surface (DOFs=780)

Comparison

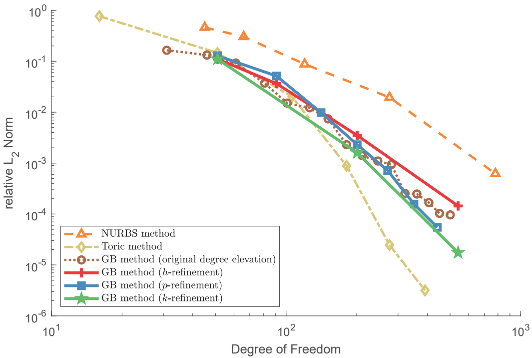

relative L_2 Norm
Degree of Freedom
10^0
10^{-1}
10^{-2}
10^{-3}
10^{-4}
10^{-5}
10^{-6}
10^1
10^2
10^3
NURBS method
Toric method
GB method (original degree elevation)
GB method (h-refinement)
GB method (p-refinement)
GB method (k-refinement)

谢 谢!

Joint with
Luis García-Puente (SHSU, USA)
Frank Sottile(TAMU, USA)
X.F. Zhu, L.Y Sun, Y. Zhang, X.Y. Zhao, H. Wang, J. Li, Y.Y. Yu, Y. Ji, M.Y. Wang, P. Zhou, ... (DUT)

Email: cgzhu@dlut.edu.cn